VIRTUAL STRINGS BASED ON A 1-D FDTD WAVEGUIDE MODEL: STABILITY, LOSSES, AND TRAVELING WAVES

CUMHUR ERKUT AND MATTI KARJALAINEN

Helsinki University of Technology
Laboratory of Acoustics and Audio Signal Processing
P.O.Box 3000, FIN-02015 HUT, Finland
Cumhur.Erkut@hut.fi
Matti.Karjalainen@hut.fi

The one-dimensional digital waveguide structures based on finite difference time domain (FDTD) formulations provide a flexible approach for real-time sound synthesis of simple one-dimensional (1-D) structures, such as a vibrating string. This paper summarizes the basic 1-D FDTD waveguide theory, carries out the stability analysis of the model, and presents a sufficient condition for the stability. The simulation of frequency-independent losses has also been covered. The formation of the traveling waves and initialization of the 1-D FDTD waveguides are investigated. The methods shown in the paper may be used to interconnect the 1-D FDTD waveguides to other model-based sound synthesis structures, such as digital waveguides that are based on the traveling wave solution of the wave equation.

INTRODUCTION

The research on model-based sound synthesis has provided novel DSP tools for emerging virtual acoustics and entertainment audio. A recent development is the formulation of one-dimensional (1-D) waveguides for improved sound synthesis using the finite differences in the time domain (FDTD) [1]. The technique is essentially a generalization of the digital waveguide mesh [2, 3] in one-dimension, and it is useful for model-based sound synthesis of 1-D structures, e.g. vibrating strings. A guitar string model has been shown to run in real-time on a typical desktop computer [1]. With the increasing computational power, in the near-term future the technique may provide an extension to the wide-spread physical modeling synthesis methods, such as digital waveguide synthesis[1] . At the present, however, the method has a broad range of problems to be solved.

The need for the stability analysis of the 1-D FDTD model has been pointed out in [1]. Moreover, it is desirable to relate the basic parameters of the model to physical quantities. A key element in the interaction of the 1-D FDTD waveguide with other models, such as DWGs, is the ability to formulate the traveling waves at any instant. In addition, the initialization of the model provides a tool for understanding of the model dynamics. These requirements are the motivations for the present paper.

The structure of the paper is as follows. After reviewing the 1-D FDTD waveguide theory in Section 1, we present the stability analysis of the model structure and derive a *sufficient condition* for the stability in Section 2. Section 3 shows the similarity of the model to the finite difference simulation of lossy wave equation. The resulting physically meaningful model parameters ensure the numerical stability. The topic of the next section is the calculation of the traveling waves and the formation of initial states of the model. Finally, in Section 5, we discuss how these methods can be applied to sound synthesis and indicate possible future directions of the research.

[1]We will refer to a digital waveguide presented in [4] as **DWG** henceforth to avoid confusion. The DWGs are based on the traveling wave solution of the wave equation, whereas 1-D FDTD waveguides do not presume the form of the solution. An excellent review of the DWG theory can be found in [5]

1. BASIC THEORY OF 1-D FDTD WAVEGUIDES

The formulation of the 1-D FDTD waveguides originates from the finite difference approximation of the wave equation in a one-dimensional lossless medium [6]:

$$y_{tt} = c^2 y_{xx} \tag{1}$$

where y is the displacement, t and x are temporal and spatial variables, respectively. The propagation speed is given by $c = \sqrt{T/\mu}$, where T is the tension of the string and μ is its linear mass density. The following central difference schemes for even order partial derivatives can be used for discretization of Eq. (1) [7]:

$$y_{tt} \approx \frac{y_{x,t+\Delta t} - 2y_{x,t} + y_{x,t-\Delta t}}{\Delta t^2} \tag{2}$$

$$y_{xx} \approx \frac{y_{x+\Delta x,t} - 2y_{x,t} + y_{x-\Delta x,t}}{\Delta x^2} \tag{3}$$

In the discrete form, the temporal and spatial variables may be denoted as $k = x/\Delta x$ and $n = t/\Delta t$, where Δt and Δx are the temporal and spatial sampling intervals, respectively. The sampling intervals cannot be chosen arbitrarily; the Von Neumann stability condition [7, 8] dictates the following constraint

$$c\frac{\Delta t}{\Delta x} \leq 1 \quad (4)$$

The choice $c = \Delta x/\Delta t$ eliminates the truncation error and numerical dispersion [7]. In this case, the term $y_{k,n}$ vanishes and the discrete solution of Eq. (1) yields

$$y_{k,n+1} = y_{k-1,n} + y_{k+1,n} - y_{k,n-1} \quad (5)$$

Note that this choice is valid in the case of an ideal string. If the medium is non-ideal, spatial oversampling may improve the simulation accuracy.
The relation $c = \Delta x/\Delta t$ is a principal condition in the DWG theory, and Eq. (5) is the one-dimensional equivalent of the $N-$dimensional rectangular DWG-mesh [3]:

$$y_{k,n+1} = \frac{1}{N}\sum_{j=1}^{2N} y_{j,n} - y_{k,n-1} \quad (6)$$

The 1-D FDTD waveguide is a generalization of the solution in Eq. (5). It has been defined as the following DSP structure [1]

$$y_{k,n+1} = g_k^+ y_{k-1,n} + g_k^- y_{k+1,n} + a_k y_{k,n-1} \quad (7)$$

In [1], it has been shown that the parameters g_k^+, g_k^-, and a_k can be used for simulating the losses, scattering and fractionally positioned terminations. However, the determination of the parameters that ensure the stability has not been carried out in the original formulation. The next section derives a sufficient condition for the stability of the 1-D FDTD model for the case $g_k^+ = g_k^- = g$.

2. STABILITY ANALYSIS OF 1-D FDTD WAVEGUIDES

The stability analysis of FDTD schemes is based on the Von Neumann analysis [8]. The method basically decomposes the states of the FDTD schemes into complex sinusoidal functions of the *spatial frequency* ξ so that the scheme can be presented by means of an *amplification function* $H(\xi)$. The necessary and sufficient condition for bounded output is that the roots λ_j of the amplification function are on or inside the unit circle.
The Von Neumann method has usually been used in FDTD simulations to determine the grid density or to analyze the numerical dispersion [7, 2, 3]. The difference in the present analysis is that we have a predetermined grid density governed by a fixed $(\Delta x, \Delta t)$ pair and we are seeking the parameters that ensure the stability of the model.
With the assumption that $g_k^+ = g_k^- = g$, and $a_k = a$, and by inserting $F(y_{k,n}) = \lambda^n e^{\imath m\theta}$ where $\theta = \Delta x\xi$ and $F(.)$ is the spatial Fourier transform operator, Eq. (7) yields

$$\lambda^2 - 2\lambda g\cos\theta - a = 0 \quad (8)$$

The roots of this quadratic equation are

$$\lambda_{1,2} = g\cos\theta \pm \sqrt{g^2\cos^2\theta + a} \quad (9)$$

In the ideal case of Eq. (5), where $g = 1$ and $a = -1$, the roots become

$$\lambda_{1,2} = \cos\theta \pm \sqrt{\cos^2\theta - 1} = \cos\theta \mp \imath\sin\theta$$

Thus

$$|\lambda_1^2| = |\lambda_2^2| = 1$$

so that the scheme is stable for all spatial frequencies. A sufficient condition for the stability of the 1-D FDTD scheme is

$$a = -g^2 \;\;,\;\; |g| \leq 1 \quad (10)$$

In this case, Eq. (9) yields

$$\lambda_{1,2} = g\cos\theta \pm \imath g\sin\theta \quad (11)$$

so that

$$|\lambda_{1,2}| = g \quad (12)$$

It is worth noting that the sufficient condition of Eq. (10) results in a frequency-independent amplification function $|H(\xi)| = g$. The condition is not necessary; there are other parameter values that result in a stable model. The stable parameter examples given in [1], which were experimentally found, exhibit slight deviations from Eq. (10). These deviations may be generalized as $a = -g^2 \pm \epsilon$ where ϵ is a small positive number. The parameter examples given in [1] correspond to $\epsilon_1 = 2.75 \times 10^{-4}$ and $\epsilon_2 = 2 \times 10^{-5}$. In both cases, the model remains passive and stable. However, since $\epsilon \neq 0$, the amplification function $H(\xi)$ exhibits humps around the DC and Nyquist frequency[2] , as discussed in [1]. Such a small offset necessarily makes the amplification function frequency dependent.

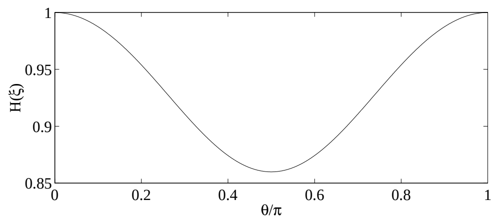

Figure 1: The magnitude of the amplification function when $g = 0.93$ and $a = -g^2 + \epsilon = -0.8599$, where $\epsilon = 0.005$. The model is passive and stable, however the amplification function is frequency-dependent.

The effect of a small offset is illustrated in Fig. 1, which presents the magnitude of the amplification function when

[2]Strictly speaking, we mean the *spatial frequency* ξ. However the relation $c = \Delta x/\Delta t$ allows the discussion to be valid for the temporal frequency ω as well.

$g = 0.93$ and $a = -g^2 + \epsilon = -0.8599$, where $\epsilon = 0.005$. The condition $|H(\xi)| \leq 1$ is satisfied, however, the frequency components around DC and Nyquist do not decay at all. The sufficient condition of Eq. (10) prevents such non-decaying components.

3. THE RELATION OF THE 1-D FDTD MODEL TO THE LOSSY WAVE EQUATION

Having established a sufficient condition for the stability in the previous section, we present the finite difference approximation of the lossy wave equation. The presentation is similar to that in [7], however our aim is to relate the 1-D FDTD model parameters to physical quantities, rather than analyzing the numerical dispersion of the scheme. The losses can be simulated by a term that is proportional to the velocity [6, 7]. In this case, the wave equation becomes

$$y_{tt} + 2b_1 y_t = c^2 y_{xx} \tag{13}$$

where $c = \sqrt{T/\mu}$, $b_1 = 1/\tau$ is a frequency-independent decay constant, and τ is the time constant for which the amplitude of the wave decays to $1/e$ of its initial value. The first order time derivative in Eq. (13) can be approximated using the following difference scheme [7]:

$$y_t = \frac{y_{k,n+1} - y_{k,n-1}}{2\Delta t} + O(\Delta t^4) \tag{14}$$

where $O(.)$ denotes the order of the approximation error. The central difference scheme is preferred to other schemes, e.g., the forward and backward differences which are $O(\Delta t^2)$ [8]. Inserting the first and second order central differences into Eq. (13), the recursion becomes in the lossy case

$$y_{k,n+1} = g\left(y_{k+1,n} + y_{k-1,n}\right) + \tilde{a} y_{k,n-1} \tag{15}$$

where

$$g = \frac{1}{1 + b_1 \Delta t} \tag{16}$$

and

$$\tilde{a} = -\frac{1 - b_1 \Delta t}{1 + b_1 \Delta t} \tag{17}$$

Eq. (15) is the special case of Eq. (7) for $g_k^+ = g_k^- = g$ and $a_k = \tilde{a}$ for all k. The parameter b_1 directly controls the decay rate of the synthetic tone.

In the following, we present an example where the sampling frequency is $f_s = 1/\Delta t = 22050$ Hz, and the fundamental frequency of the waveguide is $f = 441$ Hz. The 1-D FDTD waveguide given by Eq. (15) has been initialized with an ideal pluck (see Section 4) at the middle of the string. The initial amplitude has been set to unity. The choice $b_1 = 1$ corresponds to a decay time $\tau = 1/b_1 = 1$ s. The g and $\tilde{a}$ parameters are obtained by Eq. (16) and Eq. (17), respectively.

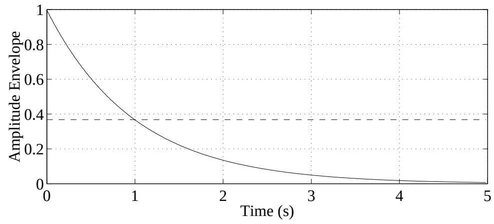

Figure 2: Lossy 1-D FDTD waveguide simulation. The synthetic tone exhibits an exponential decay and has an amplitude equal to $1/e$ at $t = \tau = 1$ s.

Figure 2 shows the amplitude envelope of the synthetic tone (only the positive part of the envelope is shown). The dashed line in the figure represents $1/e$ of the initial amplitude. The synthetic tone exhibits an exponential decay, and intersects the dashed line at $t = \tau = 1$ s.

The loss parameter $\tilde{a}$ is in agreement with the stability condition of Eq. (10)

$$\tilde{a} = -g^2 + \frac{b_1^2 \Delta t^2}{(1 + b_1 \Delta t)^2} \approx a + O(b_1^2 \Delta t^2) \tag{18}$$

where the approximation is obtained by Taylor series expansion. The neglected term is typically much smaller than the ϵ examples given in Section 2. For instance, if $b_1 = 1$ and $1/\Delta t = f_s = 22050$ Hz, the error between the a and $\tilde{a}$ is of the order 10^{-9}.

The mean-square error (MSE) between two synthetic tones obtained with a and $\tilde{a}$ is depicted in Fig. 3. The MSE is less than 10^{-9}, with a maximum at time $t = \tau$. In this case, and in all other practical cases, this error is negligible and g and $\tilde{a}$ parameters obtained by Eq. (16) and Eq. (17), respectively, result in a stable model.

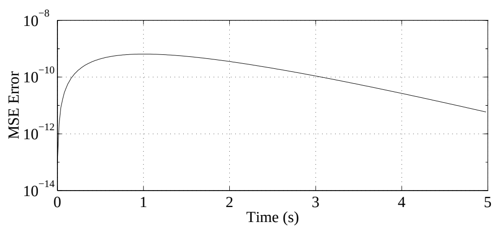

Figure 3: The mean-square error between the tones synthesized with parameter a of Eq. (10) and parameter $\tilde{a}$ of Eq. (17).

So far we discussed frequency-independent losses. The frequency-dependent losses can be simulated by inserting another loss term which is proportional to the third order time derivative in Eq. (13). In this case the difference equation becomes implicit and approximations have to be made [7]. The resulting structure is far more complex than the 1-D FDTD model, and it will not be discussed further here.

4. TRAVELING WAVES AND INITIAL STATES

The equivalence of DWG formulation and finite difference approximation in the lossless case has been previously shown in [5]. In this section we work the same problem other way around and discuss how to obtain the traveling waves in an 1-D FDTD waveguide at the time step n. We also relate the formation of initial states at $n = 0$ to this formulation. For the clarity of the discussion, we consider the lossless case, given by Eq. (5). The method outlined here can also be used for the general model of Eq. (7).
We assume that $y_{k,n-1}$ and $y_{k,n}$ are available after the calculation of $y_{k,n+1}$ for all k and n. During the discussion, we will implicitly refer to the spatio-temporal grid of the 1-D FDTD waveguide, illustrated in Fig. 4.

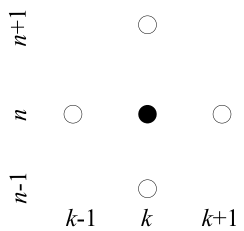

Figure 4: The spatio-temporal grid of the 1-D FDTD waveguide.

4.1. Traveling slope waves

Recall that, in the continuous case

$$\frac{\partial y(x,t)}{\partial x} = y_x^r(x-ct)+y_x^l(x+ct) = s^r(x-ct)+s^l(x+ct)$$

The superscripts r and l denote the right-going and left-going traveling waves, respectively, and $s(x,t) = y_x(x,t)$ is a slope wave in the above expression. The time derivative of the displacement is given by

$$\begin{aligned}\frac{\partial y(x,t)}{\partial t} &= y_t^r(x-ct)+y_t^l(x+ct) \\ &= c(s^l(x+ct) - s^r(x-ct))\end{aligned}$$

From this equation pair we obtain the slope waves

$$s^r(x,t) = \frac{\partial y(x,t)}{\partial x} - \frac{1}{c}\frac{\partial y(x,t)}{\partial t} \qquad (19)$$

$$s^l(x,t) = \frac{\partial y(x,t)}{\partial x} + \frac{1}{c}\frac{\partial y(x,t)}{\partial t} \qquad (20)$$

In digital simulation, spatial derivatives can be approximated by the following central difference scheme

$$y_x \approx \frac{y_{k+1,n} - y_{k-1,n}}{2\Delta x} + O(\Delta x^4) \qquad (21)$$

and time derivatives can be approximated by a similar expression previously given in Eq. (14). The digital slope waves in the lossless 1-D FDTD waveguide thus are

$$\begin{aligned} s_{k,n}^r &= \frac{y_{k+1,n} - y_{k-1,n}}{2} - \frac{y_{k,n+1} - y_{k,n-1}}{2} \\ s_{k,n}^l &= \frac{y_{k+1,n} - y_{k-1,n}}{2} + \frac{y_{k,n+1} - y_{k,n-1}}{2} \end{aligned} \qquad (22)$$

These expressions can be made explicit by inserting $y_{k,n+1}$ from Eq. (5) into Eq. (22) so that

$$\begin{aligned} s_{k,n}^r &= -y_{k-1,n} + y_{k,n-1} \\ s_{k,n}^l &= y_{k+1,n} - y_{k,n-1} \end{aligned} \qquad (23)$$

A slope wave can be converted to any other wave by means of digital operations [4]. Before demonstrating the traveling waves in the 1-D FDTD waveguide, we will discuss the initial state formation. The different initial state conditions presented below provide a generalization of the experimental cases discussed in [1].

4.2. Initial states

A second-order equation such as the wave equation needs two initial conditions. For strings, the initial displacement $y_0(x)$ and the initial velocity $v_0(x)$ provide a natural choice of the initial variables.
In an inifite string, the displacement is given by [6]

$$\begin{aligned} y(x,t) &= \frac{1}{2}\left[y_0(x-ct) + y_0(x+ct)\right] \\ &+ \frac{1}{2c}\left[S(x+ct) - S(x-ct)\right] \end{aligned} \qquad (24)$$

where

$$S(\zeta) = \int_0^{\zeta} v_0(x)dx \qquad (25)$$

In a finite string, $y_0(\zeta)$ and $S(\zeta)$ behave differently at the boundaries. For instance, at a rigid boundary $x = 0$, i.e., $\forall t$; $y(0,t) = 0$, the following conditions apply [6]

$$y_0(\zeta) = -y_0(-\zeta) \qquad (26)$$

$$S(\zeta) = S(-\zeta) \qquad (27)$$

In words, these conditions mean that the traveling waves due to $y_0(x)$ are reflected with a sign inversion at a rigid boundary, whereas the traveling waves due to $v_0(x)$ are reflected without sign inversion.
In plucked-string simulations $y_0(x)$ is usually set to an ideal triangular shape, and $v_0(x)$ is assumed to be zero.

However, measurement results indicate that a string has a non-vanishing initial velocity at the release time [9, 10]. Since the 1-D FDTD waveguide simulates the displacement of the string, for any spatially bandlimited function $y_0(x) \in L^2$ it follows that

$$y_{k,0} = y_0(x)|_{x=k\Delta x} = y_0(k\Delta x) \quad (28)$$

In words, the first initial state is the sampled initial displacement. In the following, we discuss how to set the second initial state $y_{k,-1}$ according to a given $v_0(x)$. In all the demonstrations below, the sampling frequency is $f_s = 44100$ Hz, the fundamental frequency of the string is $f_0 = 220.5$ Hz, and rigid boundary conditions are imposed.

4.2.1. Zero-velocity excitation

Consider Eq. (22) at the time $n = 0$. Since $v_0(x)$ is zero, the temporal derivatives in Eq. (22) vanish so that the slope waves satisfy

$$s^r_{k,0} = s^l_{k,0} \quad (29)$$

From Eq. (23) we get the second initial state as

$$y_{k,-1} = \frac{y_{k+1,0} + y_{k-1,0}}{2} \quad (30)$$

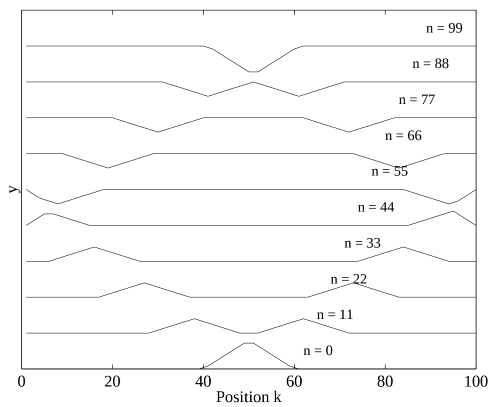

Figure 5: The displacement of the string at various time instants n. The initial displacement is a triangular function, and the initial velocity is zero.

Figure 5 represents a simulation, where $v_0(x) = 0$ and

$$y_{k,0} = \begin{cases} 1 - \frac{|k-50|}{10} & 40 \le k \le 60 \\ 0 & \text{otherwise} \end{cases} \quad (31)$$

corresponding to a triangular pulse in the middle of the string. As the simulation proceeds, two traveling waves propagate towards opposite directions. The amplitudes of the traveling waves are equal to one-half of the initial

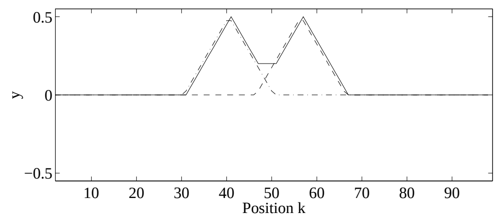

Figure 6: The traveling waves $y^r_{k,n}$ (dashed curve) and $y^l_{k,n}$ (dash-dotted curve), and the displacement $y_{k,n}$ (solid line) as calculated by the 1-D FDTD waveguide at time instant $n = 7$.

displacement. The rigid boundary conditions invert the traveling waves, in accordance with Eq. (26).

Figure 6 depicts the displacement and traveling waves at the time step $n = 7$ in the experiment above. The traveling slope waves are obtained by Eq. (23), and they are converted to the displacement waves using numerical integration (in this experiment a cumulative sum has been used). For the real-time implementation, a leaky integrator can be used to perform the integration [4].

4.2.2. Zero-displacement excitation

If $y_0(x) = 0$, Eq. (22) becomes a zero identity and it is not possible to obtain $y_{k,-1}$. Nevertheless, $v_0(x)$ can be approximated using the following forward difference scheme

$$v_0(x) = y_t|_{t=0} \approx \frac{y_{k,0} - y_{k,-1}}{\Delta t} + O(\Delta t^2) \quad (32)$$

Since $y_{k,0} = 0$, it follows that

$$y_{k,-1} \approx -\Delta t v_0(k\Delta x) \quad (33)$$

Figure 7 illustrates a simulation where the initial velocity is a smooth function (21-point Hamming window) centered at $k = 50$. The simulation begins with a zero displacement at $n = 0$. As the simulation proceeds, two traveling waves propagate towards opposite directions. In this case, traveling waves are not inverted at the boundaries, in accordance with Eq. (27).

It should also be noted that the forward difference scheme is not as accurate as the central difference scheme and the approximation error manifests itself by very low amplitude oscillations.

4.2.3. An arbitrary excitation

If both $y_0(x)$ and $v_0(x)$ are non-zero, the 1-D FDTD waveguide can be initiated by superposition of the two conditions above, i.e.,

$$\begin{aligned} y_{k,0} &= y_0(k\Delta x) \quad (34) \\ y_{k,-1} &= \frac{y_{k+1,0} + y_{k-1,0}}{2} - \Delta t v_0(k\Delta x) \end{aligned}$$

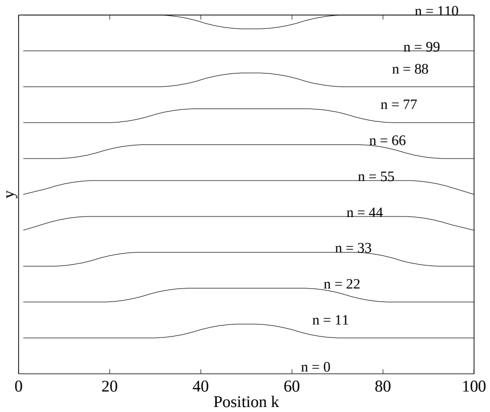

Figure 7: The displacement of the string at various time instants n. The initial displacement is zero, and the initial velocity is a Hamming function.

Figure 8 depicts the simulation results corresponding to such a case. In this simulation, the initial displacement is an ideal pluck at one third of the string, and the initial velocity has been adopted from [9]. The simulation results are in accordance with the observations presented in [9, 10].

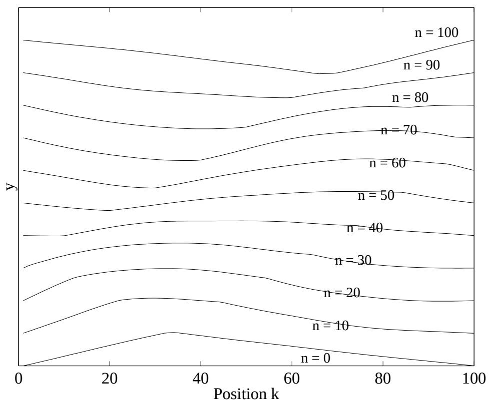

Figure 8: The displacement of the string at various time instants n. The initial displacement is an ideal pluck, and the initial velocity is a smooth function resembling the measured initial velocity in [9].

5. CONCLUSIONS

The powerful features of 1-D FDTD waveguide models have been previously introduced in [1]. The present paper documents our explorations on the mathematical theory of the method. In particular, a sufficient condition for the stability is obtained and the relation of the model parameters to the physical parameters have been demonstrated. The traveling slope waves have been formulated, and it has been shown that each traveling wave depends only on two cells in the spatio-temporal grid of the 1-D FDTD waveguide. The formation of the initial states has been related to the traveling wave formulation at $n = 0$.

One powerful aspect of the 1-D FDTD waveguide is its inherent capability to model instantaneous phenomena, such as the interactions between the string and the exciter, or nonlinearities arising from tension modulation and string-fretboard collision. These capabilities deserve proper experimentation in the near-term future.

Like many other model-based plucked string synthesis structures, 1-D FDTD waveguides produce tones that sound dull and synthetic in the absence of an instrument body model. The research on body modeling, therefore, needs to be conducted in parallel to research on the 1-D FDTD waveguide theory.

The formulation presented here may open new paths to explore the interaction between 1-D FDTD models and other model-based sound synthesis structures, e.g., DWGs. The locality of the traveling waves in Eq. (23) encourages us to work on special terminations that convert the displacement states of the 1-D FDTD waveguide to the traveling waves that can be used in DWGs, and vice versa. Using these special terminations, it will be possible to construct a hybrid model that combines the efficiency of the DWG structures with the instantaneous interaction capabilities of the 1-D FDTD waveguide. A thorough exploration of this possibility is left for future work.

6. ACKNOWLEDGMENTS

The authors wish to thank Dr. Vesa Velimäki for fruitful discussions, and to the anonymous reviewers, whose comments clarified many fine points in the paper.

REFERENCES

[1] Matti Karjalainen. 1-D digital waveguide modeling for improved sound synthesis. In *Proc. IEEE Int. Conf. Acoustics, Speech and Signal Proc.*, Orlando, Florida, USA, May 2002. Accepted for publication.

[2] S. Van Duyne and J. O. Smith. Physical modeling with the 2-D digital waveguide mesh. In *Proc. Int. Computer Music Conf.*, pages 40–47, Tokyo, Japan, 1993.

[3] L. Savioja, T. J. Rinne, and T. Takala. Simulation of room acoustics with a 3-D finite difference mesh. In *Proc. Int. Computer Music Conf.*, pages 463–466, Aarhus, Denmark, 194.

[4] Julius O. Smith. Physical modeling using digital waveguides. *Computer Music J.*, 16(4):74–91, 1992.

[5] Julius O. Smith. Principles of digital waveguide models of musical instruments. In Mark Kahrs

and Karlheinz Brandenburg, editors, *Applications of Digital Signal Processing to Audio and Acoustics*, pages 417–466. Kluwer Academic Publishers, Boston, Massachusetts, USA, 1998.

[6] P. M. Morse. *Vibration and Sound*. American Institute of Physics for the Acoustical Society of America, 1976. (1^{st} ed. 1936, 2^{nd} ed. 1948).

[7] Antoine Chaigne. On the use of finite differences for musical synthesis. Application to plucked stringed instruments. *Journal d'Acoustique*, 5(2):181–211, 1992.

[8] John C. Strikwerda. *Finite difference schemes and partial differential equations*. Wadsworth, Brooks & Cole, California, US, 1989.

[9] Maria Pavlidou and Bernard E. Richardson. The string-finger interaction in the classical guitar. In *Proc. Int. Symposium Musical Acoustics*, pages 559–564, Dourdan, France, July 1995.

[10] Maria Pavlidou and Bernard E. Richardson. The string-finger interaction in the classical guitar: theoretical model and experiments. In *Proc. Int. Symposium Musical Acoustics*, pages 55–60, Edinburgh, UK, September 1997.